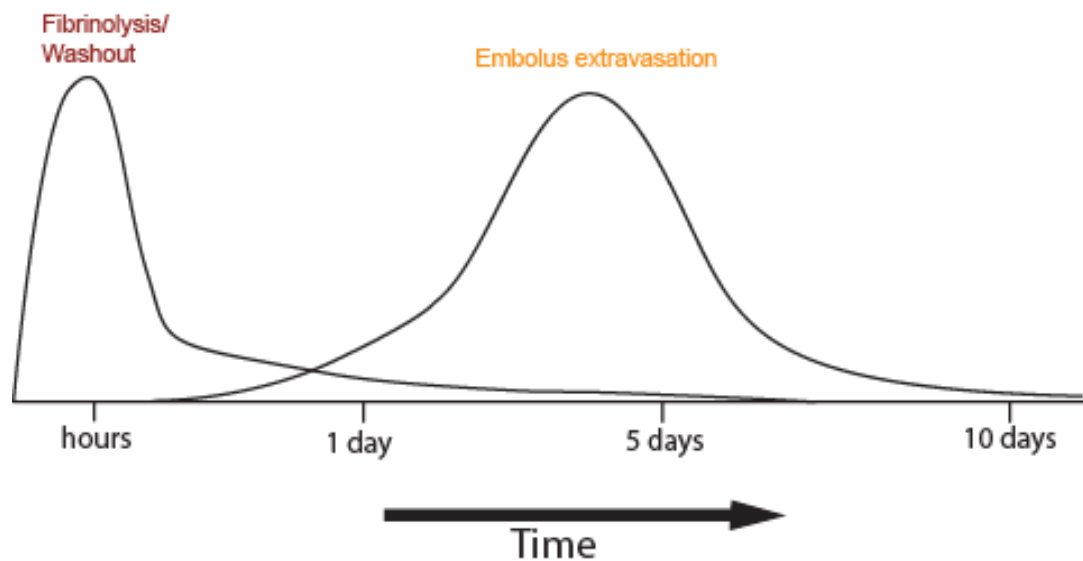
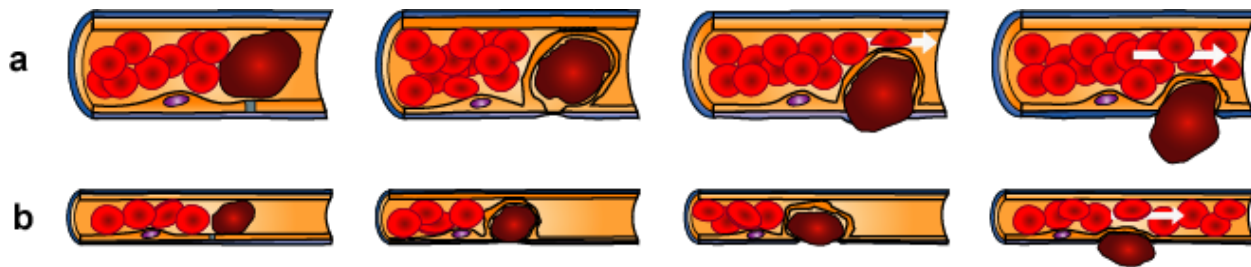


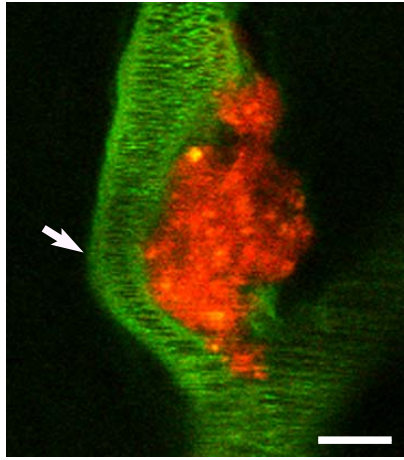
Supplementary Figure 1. Mechanism of embolus extravasation. (a) If hemodynamic forces and the fibrinolytic system fail to clear occluded microvessels within the first few hours post occlusion, their efficiency is very low for clearing vessels thereafter. The following cellular processes are then triggered: (b) Gradual extension of a membrane projection derived from the adjacent endothelium around the embolus: (c) The new membrane projection completely envelops the adjacent embolus. Cell-cell adhesion complexes are observed between the new membrane and the preexisting adjacent endothelium. These junctions we speculate may help in the guidance of the new membrane during the envelopment process and may also assure that no plasma flow occurs at this stage. (d) Matrix metalloproteases may induce tight junction and basal lamina disruption leading to the formation of an endothelial opening for embolus translocation into the perivascular parenchyma. Furthermore, MMPs may also be involved in the disruption of adhesive complexes between the new membrane and adjacent endothelium leading to their dissociation. Pericytes may induce vessel constriction, which combined with hemodynamic forces may help in extruding the emboli. (e) Once the embolus is completely enveloped by the endothelial membrane a narrow lumen is formed through which plasma and in larger arterioles some cells can flow. (f) Emboli are then extruded through the endothelial opening and the new endothelial membrane realigns to form a new vessel wall. Normal blood flow is then re-established. (g) Extravasated embolic material is gradually degraded. Possible mechanisms of degradation include microglia phagocytosis as well extravascular proteolysis of fibrin clots. Prompt embolus extravasation ultimately leads to recovery of normal blood flow and prevents microvessel damage. In aged mice however, the extravasation process is impaired leading to an overall increased brain susceptibility to microemboli manifested by vessel and synaptic degeneration.



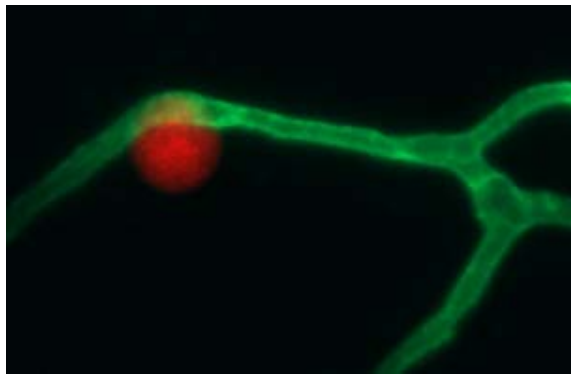
Supplementary Figure 2. Proposed time line of the various mechanisms of microvascular recanalization. The fibrinolytic system and hemodynamic forces can clear a substantial fraction of emboli (10-20 microns) within the first few hours post embolization. However, once emboli are retained in the microvasculature, these two mechanisms are very ineffective in reestablishing blood flow. Embolus extravasation occurs mostly within the next 2 to 5 days and leads to complete reestablishment of blood flow and sparing of the vessel. In addition, we also observe engulfment of smaller embolic fragments that occurs even with emboli that end up being washed out within the first 1-2 days. Thus it is possible that partial embolus engulfment and extravasation may occur rapidly after initial occlusion and may contribute to the early washout that is presumed to be solely mediated by fibrinolysis and hemodynamic forces. Embolus extravasation is likely to be even more important for clearing materials such as complex clots and cholesterol emboli, which are not susceptible to fibrinolysis.



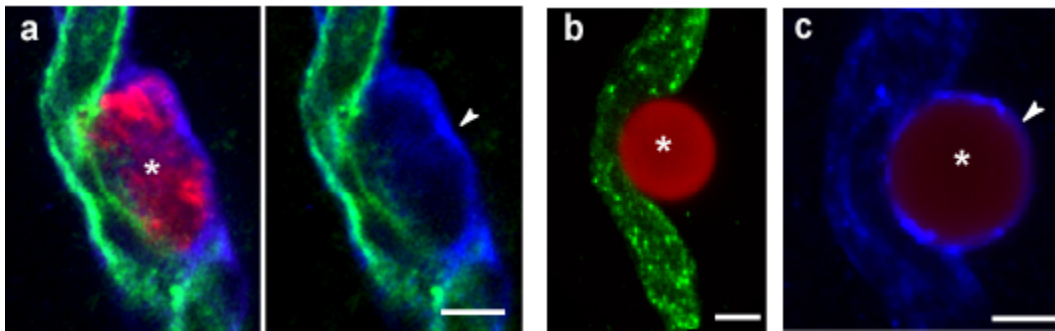
Supplementary Figure 3. Flow is reestablished rapidly during the extravasation process allowing vessel survival. (a) In arterioles $>20\ \mu\text{m}$ in diameter, blood flow is reestablished, at least partially, even before complete embolus extravasation given that multiple rows of cells can circulate simultaneously. **(b)** In capillaries, blood flow is generally reestablished following complete embolus translocation. Although flow is reestablished soon after extravasation, this doesn't mean that in every case of embolic occlusion, extravasation will occur on time for salvaging a vessel. For example, we have observed that occlusion of larger vessels (>25 microns) can in a variable number of cases lead to vessel death before recanalization occurs (depending on a variety of factors including the location of the vessels and collateral flow). This is likely to result from the lack of vascular redundancy in the perfusion of these larger areas which leads to more severe ischemia than with the occlusion of capillaries. In contrast to larger arterioles, in smaller ones (10-15 microns), extravasation appears to be very effective in salvaging the vessel given that we almost never see the degeneration of a vessel occluded by emboli of such small size.



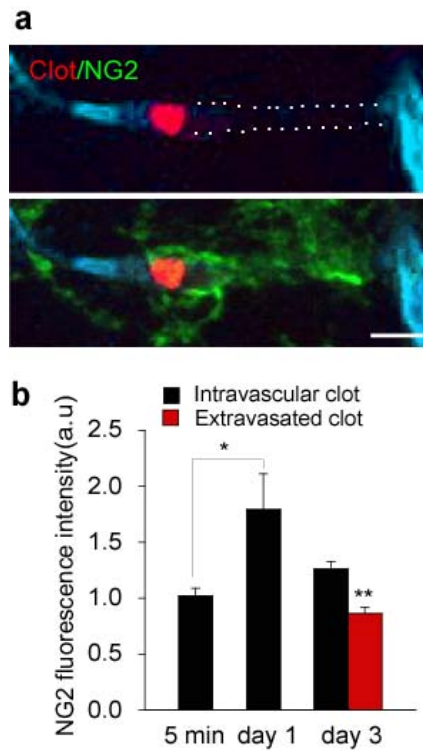
Supplementary Figure 4. Flow is reestablished gradually during the extravasation process. In vivo TPM image of a fibrin clot in the process of extravasation 2 days post-embolization. Partial vascular recanalization is already present as evidenced by the typical pattern of moving blood cells (dark lines within the thioflavin-s-labeled plasma; white arrow). (Supplementary movie 4). Scale Bar: 10 μ m.



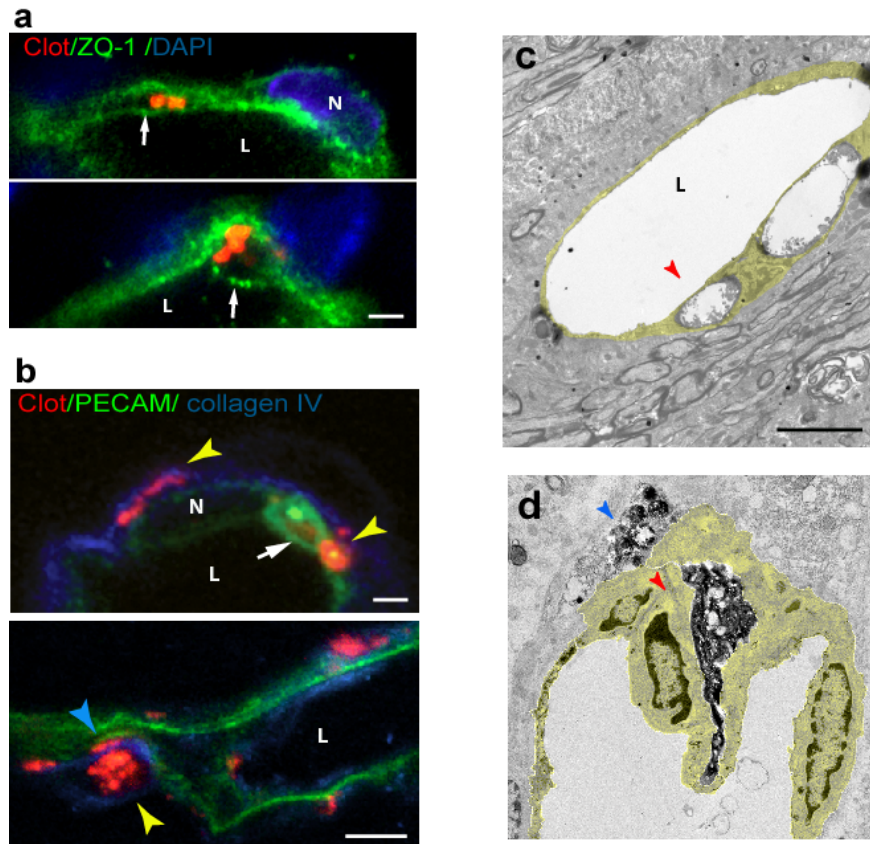
Supplementary Figure 5. Embolus extravasation in capillaries and small microarterioles almost invariably leads to vessel sparing. To determine the efficiency of flow reestablishment once emboli are extravasated, we infused mice with 15 micron microspheres (red) and 2 weeks later we injected them with a fluorescent intravascular dye (green) (lycopersicom esculentum lectin or thioflavin -S) to label the vessel prior to sacrifice. We obtained confocal images of 200 microspheres in 6 mice. Only in 5/200 cases we observed microspheres which were not associated with any vessel labeling immediately next to them. In contrast, in 195/200 cases we observed a well labeled vessel, adjacent to extravasated microspheres (red) suggesting that in the vast majority of occlusions in vessels of this caliber, flow is successfully regained after extravasation and vessels are spared.



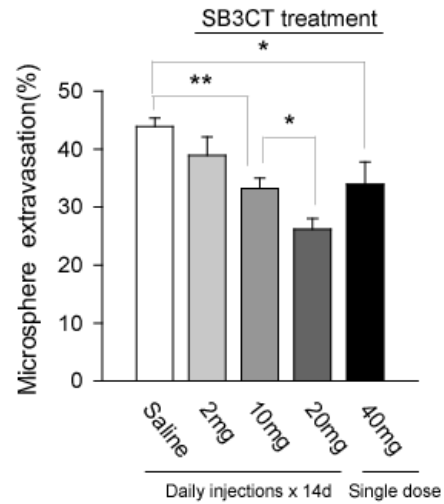
Supplementary Figure 6. Extracellular matrix remodeling occurs during the extravasation process. Confocal image of fluorescently conjugated fibrin clot (asterisk) which is located outside the collagen IV (blue) immunolabeled basal lamina (white arrowhead). **a**, Confocal image shows a cholesterol embolus (asterisk) located outside the PECAM-1 immunolabeled endothelium (green) and surrounded by collagen IV immunolabeled basal lamina (blue, white arrowhead). **b**, Confocal image of a polystyrene microsphere located outside the PECAM-1 immunolabeled endothelial membrane (green). **c**, a microsphere is shown entirely outside the vascular basal lamina and surrounded by a layer of collagen IV. Scale bars 5 μ m.



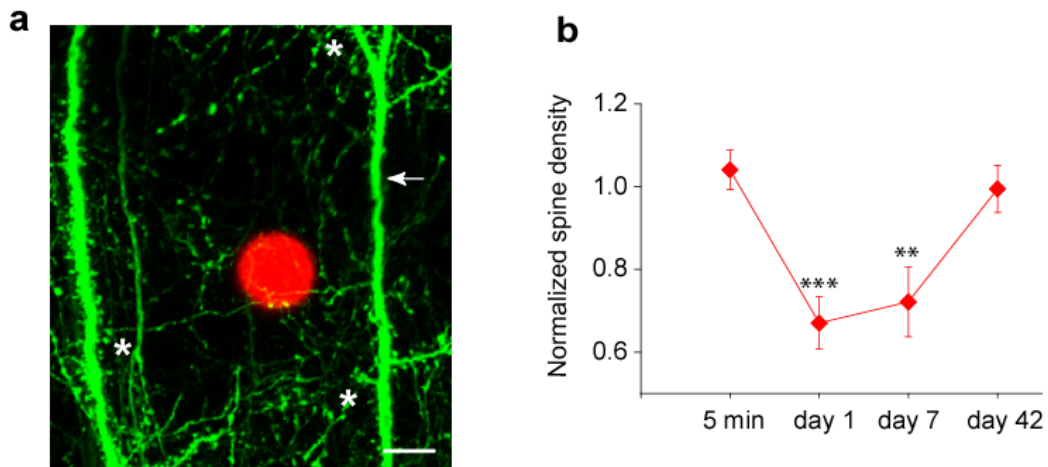
Supplementary Figure 7. Pericyte hypertrophy in the vicinity of emboli occlusion. a, NG2-immunoreactive pericyte processes (green, bottom panel) wrapping around a fibrin clot (red) and occluded capillary. Note the diminished intravascular dye (dotted line, top panel) suggesting vessel constriction. Scale bar 15 μ m. **b,** Quantification of NG2 immunofluorescence intensity around microvessels containing intravascular versus extravasated clots at different time intervals (mean \pm s.e.m; n=8 mice and 44 blood vessels, * p<0.05, One way ANOVA, **p<0.01 two-tail Student's t-test).



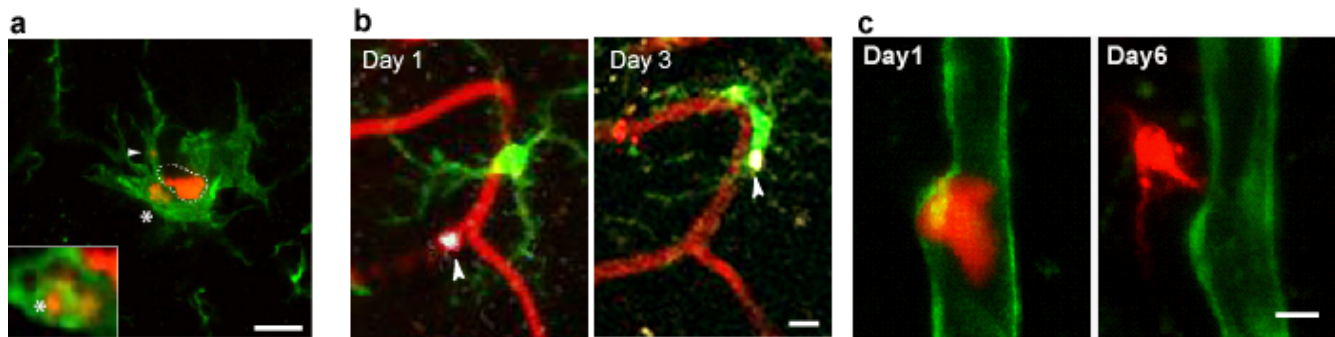
Supplementary Figure 8. Envelopment and extravasation of small embolic fragments. **a**, Confocal images of ZO-1 immunolabeled microvessels delineate the luminal and abluminal endothelial membranes revealing fibrin clot fragments (red) enveloped by endothelial membranes (white arrows). DAPI labeling (blue) highlights the adjacent endothelial nucleus (N). Scale bars 2 μ m. **b**, Confocal images of double immunofluorescence labeling for the endothelial marker PECAM-1 (green) and extravascular basal lamina protein Collagen IV (blue). A Clot fragment (red) is found within an endothelial compartment (white arrow, upper panel). Clot fragments are also found at various stages of extravasation and some are embedded within the basal lamina (yellow arrowheads, top and bottom panels). Scale bars 4 μ m. **c**, Transmission electron microscopy (TEM) of fibrin clots conjugated to polystyrene nanoparticles (48 nm in diameter) demonstrates the presence of clot fragments within large endothelial vacuolar compartments (red arrowhead). **d**, TEM shows a colloidal carbon-labeled fibrin clot outside of the lumen (L) but fully enveloped by endothelial membranes (red arrowhead). A clot fragment (blue arrowhead) has translocated to the perivascular space. (Endothelial boundaries are pseudocolored yellow). Scale bars, 2 μ m.



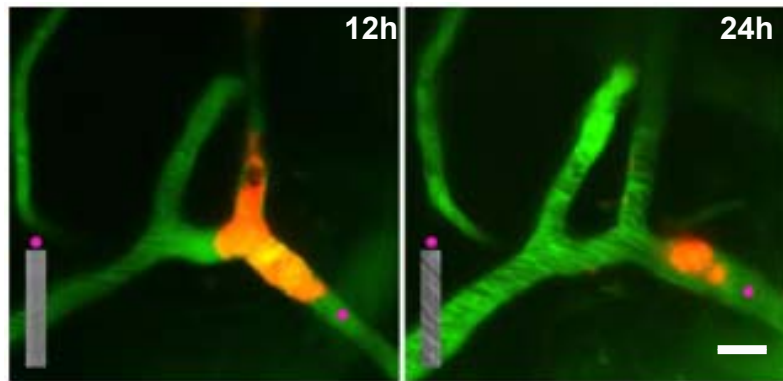
Supplementary Figure 9. Matrix metalloprotease 2/9 inhibitor SB-3CT reduces extravasation rates in a dose-dependent manner. Microsphere extravasation was examined in fixed brain slices of mice treated with SB-3CT intraperitoneally at various doses for 14 days. Microspheres are more suitable than clots for this particular quantification given their uniform size, shape and properties. (n=22 mice and ~5000 microspheres).



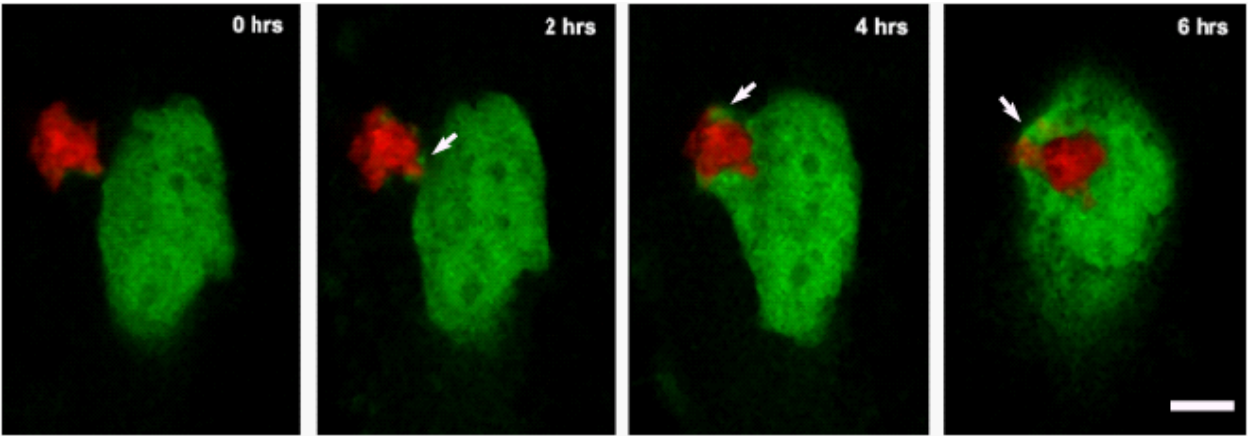
Supplementary Figure 10. Focal reversible dendritic spine loss near the occlusion. **a**, Confocal images of dendrites in mice expressing yellow fluorescent protein in neurons (green) demonstrate spine loss near vascular occlusion (arrow) but sparing of spines in areas further from the occlusion site (asterisk). Scale bar 10 μ m. **b**, Dendritic spines along YFP-labeled dendrites immediately adjacent to occluded vessels were quantified and normalized to the average spine count in distal and proximal segments of the same dendritic branch (mean \pm s.e.m.; n=12 mice, ~5000 spines. **p<0.01 and ***p<0.001, One way ANOVA).



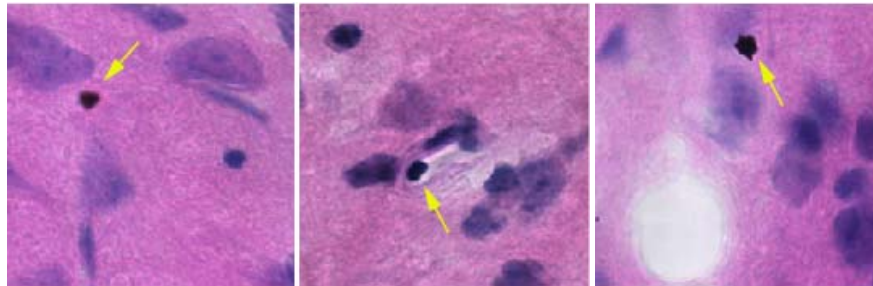
Supplementary figure 11. Microglia are capable of engulfing extravasated fibrin clots. **a**; Confocal images of IBA1 labeled microglia (green) surrounding an intravascular clot (dotted line) show that fragments of the clot (red) that have extravasated are now contained within what appear to be microglial intracellular vesicular compartments (arrowhead and asterisks). **b**; In vivo two photon imaging of a fibrin clot (pseudocolored white. Clots are labeled by conjugation with blue fluorescent 40nm nanoparticles) occluded capillary shows that 3 days post embolization the clot is now located outside the recanalized vessel and has been engulfed by an adjacent microglia (green). For this experiment mice with GFP-labeled microglia were used (see methods) and vessels were labeled by IV injection of Rhodamine dextran. **c**, in vivo time lapse image in Tie2-GFP mice shows a Texas red conjugated fibrin clot that has completely translocated outside the GFP labeled endothelium (Day 6) and appears to be contained within a cell with multiple processes (possibly a microglia). Given that only 13.5% of microvessels with extravasated clots show clot fragments within microglia (3 mice and 59 vessels), it is likely that microglia engulfment is only one of the mechanisms involved in clot degradation following extravasation. Although we never found engulfed clot material within GFAP-labeled astrocytes (data not shown), they and other perivascular cells can secrete proteolytic enzymes that could be involved in the extracellular degradation of clots. Moreover, given that clots can be directly engulfed by endothelial cells (Figure 2) and these cells are known to produce proteolytic enzymes such as tissue plasminogen activator, it is possible that substantial clot degradation could occur directly within endothelial cells even before they translocate to the brain parenchyma. Scale bars 10um



Supplementary Figure 12. Fibrin clot lysis and washout. In vivo time lapse two photon imaging of cortical microvessels (green, intravascular thioflavin-S dye) and a fluorescently conjugated fibrin clot (orange). Clot completely obstructs blood flow at 12 hours as evidenced by the absence of the characteristic flow pattern seen by line scan imaging (pink dot, left panel). At 24 hours the clot appears fragmented and much smaller but has not extravasated and blood flow is partially reestablished (pink dot, right panel). Scale bar: 10 μ m.



Supplementary Figure 13. Rapid clot envelopment by human endothelial vascular cells (HUVEC) in vitro. Time lapse two photon imaging demonstrates the capacity of HUVEC cells to rapidly generate membrane projections (white arrows) that envelop an adjacent fluorescent fibrin clot (red) in a process that resembles the one observed in vivo. Scale bar: 10 μ m.



Supplementary figure 14. Visualization of fibrin clots in hematoxylin/eosin stained brain slices. Unstained fibrin microclots are invisible under conventional H/E staining (data not shown). Clots pre-stained with India ink were visualized after H/E stain (yellow arrows); however, even in this case it is very difficult to determine if clots are located inside or outside of a microvessel. We hypothesize that this difficulty in visualizing microclots by conventional histopathological analysis is one of the reasons why the extravasation phenomenon has never been reported in human postmortem brain. Scale bar 20 μ m

MOVIE LEGENDS

Movie 1. Embolus in the process of extravasation. 3D rendering of a stack of optical planes obtained in vivo by two photon microscopy in a tie2-GFP mouse (same data as figure 2 b, b" in the manuscript). A fibrin clot (red) is being extruded through an opening in the GFP-labeled microvascular endothelium (blue arrowhead). The intraluminal side of the clot is completely enveloped by a new endothelial membrane (purple arrowhead). Scale bar (see figure 2 b,b").

Movie 2. Embolus extravasation and reestablishment of blood flow. In vivo TPM time lapse imaging of thioflavin-S labeled blood vessel (green) on days 2 and 8 postembolization with fibrin clots. Image stack on day 2 (left panel) shows an embolus (red) that is partially occluding a microarteriole. A reduced blood flow is reflected in the pattern of slow cell movement observed. On day 8 (right panel) the embolus is completely outside the vessel lumen and the cell flow velocity has increased dramatically indicating that the vessel has recanalized.

Movie 3. Microsphere extravasation. 3D rendering of a confocal stack of a microvessel containing intravascular thioflavin-s (green). A microsphere (red) has extravasated completely and the vessel lumen has been completely reestablished as evidenced by its normal diameter.

Movie 4. Early extravasation and reestablishment of blood flow. TPM time lapse image stack of thioflavin-S labeled blood vessel (green) on day 2 postembolization with cholesterol emboli. The embolus (red) is shown at a very early stage of extravasation. Although the embolus has not yet translocated completely outside the vessel, blood flow has been diverted around the embolus through a narrow space (yellow arrowhead). A smaller embolus (blue arrowhead) has been completely extravasated.

Movie 5. Cholesterol embolus occlusion. In vivo TPM image stack of thioflavin-S labeled blood vessel (green), 24 hours postembolization with cholesterol emboli (red). In flowing vessels the intravascular dye creates moving diagonal scanning patterns whereas in occluded vessels (arrowhead) a solid non-moving column of dyed plasma is seen.